

## **Influence of Electrodeposited Ni-Mo Alloy on Hydrogen Evolution Reaction at Nickel Foam Cathode**

*Tomasz Mikolajczyk\**, *Boguslaw Pierozynski*

Department of Chemistry, Faculty of Environmental Management and Agriculture, University of Warmia and Mazury in Olsztyn, Plac Lodzki 4, 10-727 Olsztyn, Poland

\*E-mail: [tomasz.mikolajczyk@uwm.edu.pl](mailto:tomasz.mikolajczyk@uwm.edu.pl)

*Received:* 5 October 2017 / *Accepted:* 22 November 2017 / *Published:* 16 December 2017

---

This communication covers an electrochemical investigation of hydrogen evolution reaction (HER), studied at unmodified (pure) Ni foam and Ni foam modified by MoNi alloy deposit. The quantity of electrodeposited Mo on nickel foam was derived by scanning electron microscopy (SEM) technique, combined with Energy Dispersive X-Ray spectroscopy (EDX) analysis. Kinetics of the HER were studied at room temperature in 0.1 M NaOH for the cathodic overpotential range of 100-400 mV. The electrochemical parameters for examined catalyst materials were recorded based on a.c. impedance spectroscopy and Tafel polarization techniques.

---

**Keywords:** Nickel foam; HER; MoNi alloy; Electrochemical impedance spectroscopy

### **1. INTRODUCTION**

One of the most important topics of sustainable development is the concept of “pure energy”. Extensive research activities have been carried out in order to find the most suitable fuel for the generation of “energy of the future”. A supreme example of “pure energy” carriers is hydrogen, because its oxidation (e.g. in Proton-Exchange Membrane Fuel Cells: PEMFCs) leads only to the formation of water. However, hydrogen used in fuel cells needs to be of extremely high purity, e.g. as that generated via alkaline or PEM water electrolysis [1-9].

Nevertheless, with the intention of making this technology practical, the electrochemical process should be based on the application of renewable energy sources, such as solar or hydro-energy [10-12]. Although the electrochemical generation of hydrogen has significant benefits, the process of water electrolysis remains quite expensive. The above is mostly caused by the insufficient catalytic activity of currently available cathode materials, as well as lack of cheap and commonly available, renewable energy sources. In order to improve the process of water electrolysis, extensive efforts are

being made to develop efficient and durable electrode entities (especially cathodes). Many hydrogen evolution reaction studies have shown that suitable catalytic materials for making such electrodes are based on nickel structures, including: nickel-coated carbon fibre/felt [13-16], Ni-sintered nanoparticle materials [17-19] and electrocatalysts based on nickel foam [20, 21]. In addition, these materials possess large specific surface areas; they are also highly corrosion-resistant in alkaline media and relatively inexpensive. Also, considerable enhancement of electrocatalytic properties for Ni foam materials could be achieved through the surface deposition of various nano-structured catalysts, including metal alloys and their oxides. The above might be conducted by means of electrodeposition, spontaneous deposition, chemical reduction and physical vapour deposition (PVD) methods [22].

## 2. EXPERIMENTAL

In this study, water for all solutions came from a Millipore purification system (Millipore Direct-Q3 UV) with 18.2 M $\Omega$  cm final water resistivity. Working electrolyte - 0.1 M NaOH was prepared from AESAR, 99.996% NaOH pellets of semiconductor grade. Before conducting experiments, the base solution was subjected to atmospheric air removal by bubbling with high-purity argon (Ar 6.0 grade, Linde).

**Table 1.** Composition and operating parameters used for electrodeposition of Ni-Mo alloy onto Ni foam.

Bath constituents	Amount (g L <sup>-1</sup> )	Operating parameters
Na <sub>2</sub> MoO <sub>4</sub> ×2H <sub>2</sub> O	20	Anode: Pt wire Cathode: Ni foam pH: 4.0 Temperature: 303 K Deposition time: 2 min Current density: 10 mA cm <sup>-2</sup>
NiSO <sub>4</sub> ×6H <sub>2</sub> O	90	
C <sub>6</sub> H <sub>8</sub> O <sub>7</sub> (citric acid)	40	
C <sub>6</sub> H <sub>11</sub> O <sub>7</sub> Na (sodium gluconate)	150	
Na <sub>3</sub> C <sub>6</sub> H <sub>5</sub> O <sub>7</sub> (trisodium citrate)	50	

An electrochemical cell used to perform experiments contained a working electrode (WE) in a central part, a reference (reversible hydrogen electrode; RHE) and a counter electrode (CE), both placed in separate compartments; electrodes were made of Ni foam, Pd and Pt, correspondingly. Nickel foam was brought by MTI Corporation (with surface density: 346 g m<sup>-2</sup>; thickness: 1.6 mm; purity: > 99.99 % Ni; porosity: ≥ 95 %), where for better reproductivity all examined Ni foam electrodes were cut into squares of 1 cm<sup>2</sup> (ca. 35 mg mass). Active surface area of unmodified Ni foam and MoNi-modified Ni foam was estimated from the commonly used double-layer capacitance value of 20  $\mu$ F cm<sup>-2</sup> for smooth and homogeneous surfaces [23, 24], which resulted in 14.0 and 390.0 cm<sup>2</sup>, correspondingly. Electrochemical deposition of binary MoNi alloy catalyst on nickel foam samples was carried out from electrolytic bath presented in Table 1, at a cathodic current-density of 10 mA cm<sup>-2</sup>

<sup>2</sup> to produce catalyst deposit at *ca.* 8.5 wt.% MoNi (with a ratio about 1:1) [25]. However, we were unable to clearly identify the crystallites of MoNi alloy. Thus, we could not calculate the average grain size of the catalytic deposit. Based on the literature we concluded that MoNi alloy was deposited as an amorphous structure [26].

In this study, the *Solartron* 12,608 W Full Electrochemical System (1260 frequency response analyser and 1287 electrochemical interface units) was employed for conducting electrochemical experiments. Techniques used for the HER characterisation included: a.c. impedance spectroscopy and quasi steady-state Tafel polarization. All information concerning other procedures, including specific pre-treatments employed to the WE, RHE, CE electrodes and protocols for electrochemical measurements, have recently been deliberated in other articles from this laboratory [27, 28].

Besides, a scanning electron microscope (SEM) FE-SEM Merlin unit with XFlash 5010 Bruker EDX compartment was employed for spectroscopic characterization of prepared electrodes.

### 3. RESULTS AND DISCUSSION

#### 3.1. SEM and EDX characterization of MoNi-modified Ni foam electrode

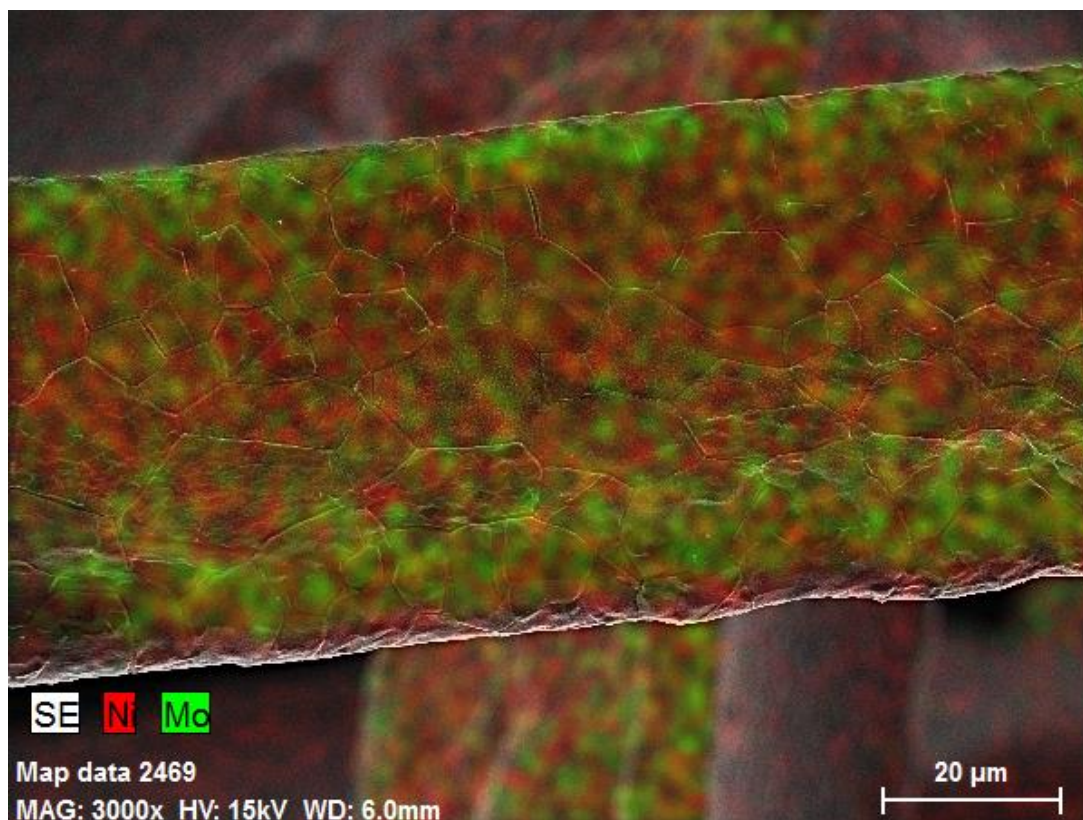


**Figure 1.** SEM micrograph picture with EDX mapping of MoNi-modified Ni foam electrode, taken at 3,000 $\times$  magnification.

Fig. 1 illustrates the arrangement of deposited MoNi alloy on the MTI foam, recorded at a magnification of 3,000 $\times$ . While this method does not provide the possibility to differentiate between

nickel atoms from Ni foam and those of the MoNi alloy, it is possible to conclude, based on the arrangement of the Mo deposit that the electrodeposition of MoNi alloy is quite homogenous all over the nickel foam surface. Fig. 2 presents an EDX spectrum for MoNi-modified Ni foam surface, which allowed to calculate the average value of Mo content at the level of 4.1 wt.%, which is in good agreement with the value estimated from the Faraday's law (3.8 wt.%).

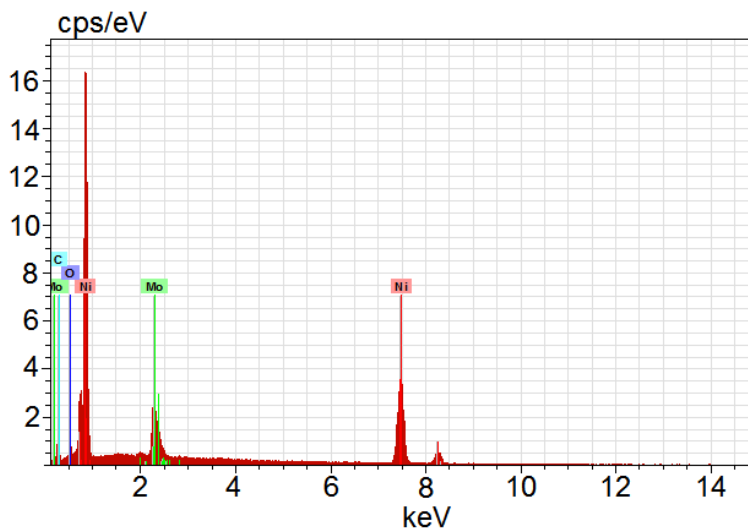


**Figure 2.** EDX spectrum for MoNi-modified Ni foam surface.

3.2. Hydrogen evolution reaction on pure and MoNi-modified Ni foam electrodes in 0.1 M NaOH

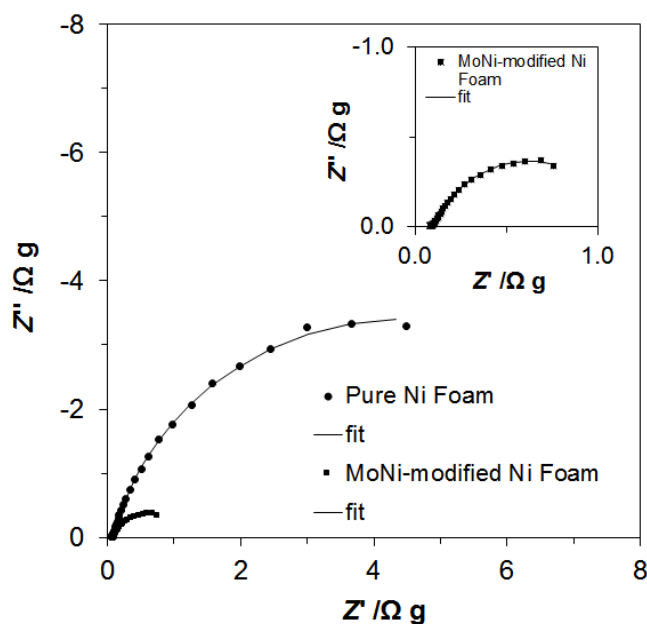


**Figure 3.** Complex-plane Nyquist impedance plots for the HER recorded on pure and MoNi-modified Ni foam electrodes in contact with 0.1 M NaOH solution (carried-out at room temperature for the overpotential of 50 mV). The solid lines correspond to a representation of the data according to the equivalent circuits shown in Figure 4, whereas points are experimental results.

A.c. impedance behaviour of the HER on unmodified and MoNi-modified Ni foam electrodes in 0.1 M NaOH solution is shown in Fig. 3 and Table 2. Here, pure Ni foam displayed single, “depressed” semicircles (a single-step charge-transfer reaction) at all studied potentials. The HER impedance parameters for unmodified Ni foam electrode were derived based on a constant phase element – CPE-modified Randles equivalent circuit model shown in Fig. 4a. The CPE element was used in the circuit in order to account for the capacitance dispersion [29, 30] effect (represented by distorted semicircles in the Nyquist impedance plots).

**Table 2.** Electrochemical parameters for the HER, obtained on pure Ni foam and MoNi-modified Ni foam electrodes in contact with 0.1 M NaOH. The results were derived by fitting the CPE-modified Randles (Figure 4a) and the two CPE-R elements (Figure 4b) equivalent circuits to the experimentally obtained impedance data (reproducibility typically below 10 %,  $\chi^2 = 4 \times 10^{-5}$  to  $2 \times 10^{-3}$ ).

$\eta/\text{mV}$	$R_{ct}/\Omega \text{ g}$	$C_{dl}/\mu\text{F g}^{-1}\text{s}^{\phi-1}$		
<b>Pure Ni foam</b>				
50	$14.78 \pm 0.15$	$7,768 \pm 96$		
100	$8.61 \pm 0.10$	$6,663 \pm 87$		
150	$3.07 \pm 0.04$	$5,253 \pm 85$		
200	$1.17 \pm 0.02$	$4,367 \pm 121$		
250	$0.84 \pm 0.02$	$3,622 \pm 172$		
300	$0.40 \pm 0.01$	$2,893 \pm 222$		
350	$0.34 \pm 0.01$	$2,165 \pm 164$		
400	$0.19 \pm 0.00$	$2,957 \pm 154$		
$\eta/\text{mV}$	$R_{ct}/\Omega \text{ g}$	$C_{dl}/\mu\text{F g}^{-1}\text{s}^{\phi-1}$	$R_p/\Omega \text{ g}$	$C_p/\mu\text{F g}^{-1}\text{s}^{\phi-1}$
<b>MoNi-modified Ni foam</b>				
50	$1.01 \pm 0.01$	$203,505 \pm 5,861$	$0.05 \pm 0.00$	$91,568 \pm 4,899$
100	$0.81 \pm 0.03$	$180,023 \pm 10,855$	$0.06 \pm 0.00$	$94,047 \pm 2,295$
150	$0.60 \pm 0.01$	$173,607 \pm 5,243$	$0.05 \pm 0.00$	$83,984 \pm 4,460$
200	$0.45 \pm 0.01$	$151,161 \pm 5,578$	$0.05 \pm 0.00$	$85,695 \pm 4,619$
250	$0.35 \pm 0.01$	$141,305 \pm 6,302$	$0.04 \pm 0.00$	$63,201 \pm 3,362$
300	$0.25 \pm 0.00$	$143,094 \pm 7,112$	$0.04 \pm 0.00$	$78,310 \pm 3,109$
350	$0.19 \pm 0.01$	$130,247 \pm 7,125$	$0.05 \pm 0.00$	$79,258 \pm 3,575$
400	$0.16 \pm 0.00$	$117,138 \pm 4,721$	$0.04 \pm 0.00$	$80,474 \pm 3,775$

Hence, for the unmodified Ni foam electrodes, the recorded Faradaic reaction resistance ( $R_{ct}$ ) parameter decreased from  $14.78 \Omega \text{ g}$  at 50 mV to  $0.19 \Omega \text{ g}$  at the overpotential of 400 mV. At the same time, the double-layer capacitance ( $C_{dl}$ ) parameter diminished from 7,768 to 2,957  $\mu\text{F g}^{-1}\text{s}^{\phi 1-1}$  for analogous overpotential range, which could be explained by partial blocking of electrochemically active electrode surface caused by insufficient desorption of hydrogen bubbles, especially observed at increased overpotentials.

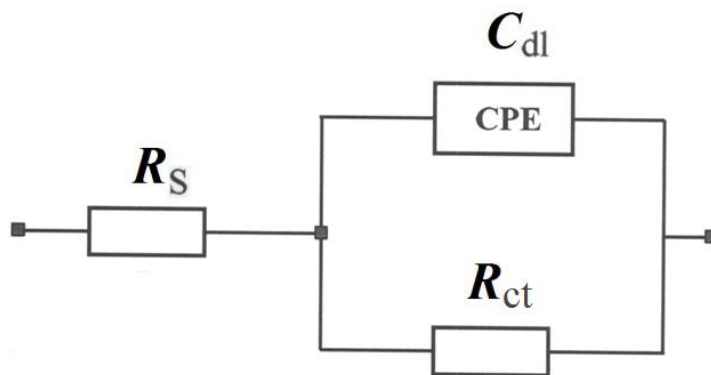


Fig. 4 a

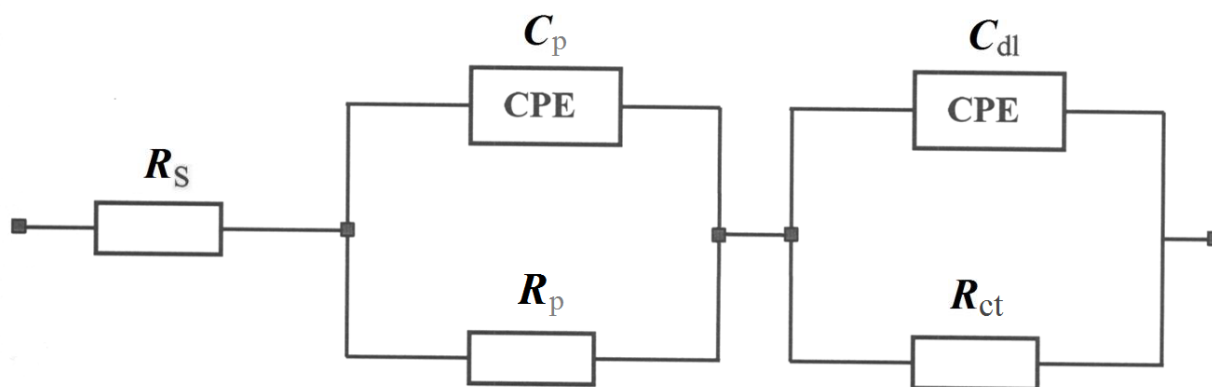


Fig. 4 b

**Figure 4.** a) Equivalent circuit used in ac impedance data modelling for pure Ni foam electrodes, conducted in 0.1 M NaOH. The circuit contains a constant phase element (CPE) for distributed capacitance; the parameters of double-layer capacitance and the HER charge-transfer resistance are expressed by  $C_{dl}$  (as CPE) and  $R_{ct}$ , while  $R_s$  is solution resistance; b) the impedance data for MoNi-modified Ni foam electrodes were fitted using a circuit model, which contained two CPE- $R$  element pairs. The circuit takes into account the porosity response from the electrode characterized by the porosity resistance and pseudo-capacitance;  $R_p$  and  $C_p$  (as CPE), parameters.

In contrast, the HER electrochemical results for the MoNi-modified Ni foam electrodes exhibited two “depressed”, partial semicircles at all examined potentials. Thus, a circuit model used for fitting the data contained two CPE- $R$  elements (Fig. 4b). The high-frequency semicircle ( $C_p$ - $R_p$ ) is typically overpotential independent and corresponds to the porosity of the electrode, whereas the low-frequency semicircle ( $C_{dl}$ - $R_{ct}$ ) is related to the kinetics of the hydrogen evolution reaction [16-19, 24].

Therefore, the  $R_{ct}$  parameter for the MoNi-modified Ni foam electrodes diminished from 1.01 to 0.16  $\Omega$  g for the overpotential span of 50-400 mV. Simultaneously, the values of the  $C_{dl}$  parameter also reduced with increasing overpotential from 203,505 to 117,138  $\mu\text{F g}^{-1}\text{s}^{\varphi 2-1}$ , correspondingly for 50 and 400 mV vs. RHE.

The modification of Ni foam by electrodeposition of the MoNi alloy caused considerable reduction of the  $R_{ct}$  parameter compared to the unmodified electrode, specifically by *ca.* 15 $\times$  at the overpotential of 50 mV. However, along with increasing overpotential, the difference between the  $R_{ct}$  parameter for the two electrodes tend to diminish and reach an almost constant value at the potential of -400 mV. The latter most likely results from the fact that the system eventually moves into the diffusion limitation control. Furthermore, deposition of most likely amorphous [26, 31] catalytic MoNi alloy resulted in significant expansion of the electrochemically accessible surface area, namely by about 26 $\times$ , as compared to the baseline Ni foam electrode, at the onset overpotential value of 50 mV.

In contrast, the high-frequency semicircle (surface porosity impedance response) was quite potential-independent, which led to a rather constant value of the  $R_p$  parameter: *ca.* 0.04-0.05  $\Omega$  g for the MoNi-modified Ni foam electrode (also refer to the respective values of pseudocapacitance parameter,  $C_p$  recorded in Table 2) over the studied overpotential range: 50-400 mV. Moreover, dimensionless  $\varphi_1$ ,  $\varphi_2$  and  $\varphi_3$  parameters ( $\varphi$  determines the constant phase angle in the complex-plane plot and  $0 \leq \varphi \leq 1$ ) of the CPE circuits (see Figs. 4a and 4b) varied between 0.82-0.98, 0.88-0.99 and 0.54-0.75, correspondingly.

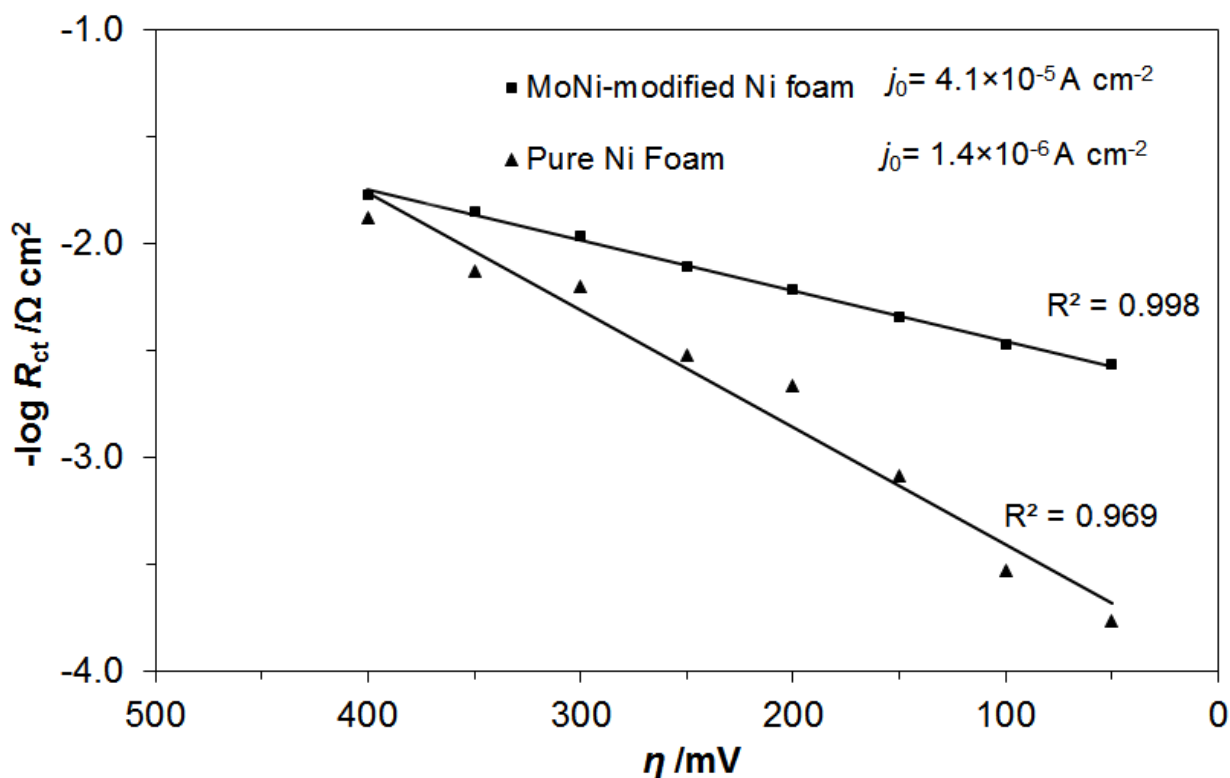


**Figure 5.**  $-\log R_{ct}$  vs. overpotential relationship, obtained for the HER performance on pure and MoNi-modified Ni foam electrodes.

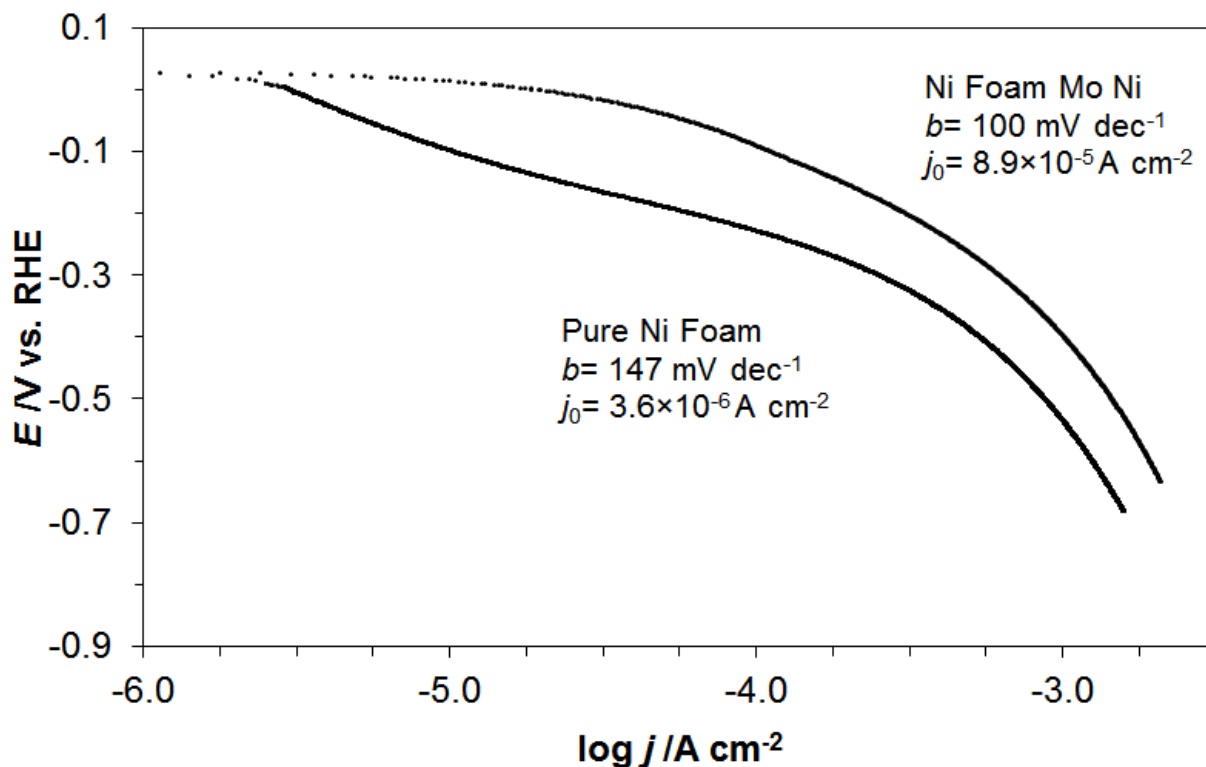


**Figure 6.** Quasi-potentiostatic cathodic Tafel polarization curves (recorded at a rate of  $0.5 \text{ mV s}^{-1}$ ) for pure and MoNi-modified Ni foam electrodes in contact with  $0.1 \text{ M NaOH}$  solution.

Based on the linear dependence of  $-\log R_{ct}$  vs. overpotential (Fig. 5), displayed here over the examined overpotential span:  $50\text{-}400 \text{ mV}$ , the exchange current-densities for the HER were calculated based on the Butler-Volmer equation and through utilization of the relation between the exchange current-density ( $j_0$ ) and the  $R_{ct}$  parameter for overpotential approaching zero value [5, 32-34]. Therefore, the calculated values of the  $j_0$  came to  $1.4 \times 10^{-6}$  and  $4.1 \times 10^{-5} \text{ A cm}^{-2}$  for the unmodified Ni foam and the MoNi-modified nickel foam catalyst materials, correspondingly.

The kinetic results discussed above were in good agreement with these of the potentiostatic Tafel polarizations, presented in Fig. 6. In fact, significant improvement of the HER behaviour upon introduction of catalytic amounts of MoNi alloy into the Ni foam structure could be observed over the kinetically-controlled, low/medium overpotential region of Fig. 6. Therefore, the Tafel-based values of the  $j_0$  parameter for the HER came to  $3.6 \times 10^{-6}$  and  $8.9 \times 10^{-5} \text{ A cm}^{-2}$  for the unmodified Ni foam and the MoNi-modified nickel foam catalyst materials with cathodic Tafel  $b$  slope equal to  $147$  and  $100 \text{ mV dec}^{-1}$ , respectively.

In fact, the recorded in this work exchange current-densities compare quite well with those of other HER works (see selected articles on the HER, performed on a similar MoNi alloy in Refs. [26, 35-40]). Nevertheless, as for some of these publications [39, 40], the results were referred to the base (unmodified) geometric surface area of the catalyst material, the recorded there  $j_0$  values were unnaturally high. The best visualisation of this practice could be observed in Refs. 36 and 38, where authors showed two types of the  $j_0$  parameter, where the first one excludes and the other one does include the roughness factor of the electrode. The above resulted in a ratio between the recorded  $j_0$

parameters reaching 10,000× (see Table 3). In contrast, the values of the  $j_0$  parameter recorded in this study were “normalized” based on the surface area estimated from the double-layer capacitance measurements (see an Experimental part for details).

**Table 3.** Comparison of the HER exchange current density values derived from the literature for electrodes containing MoNi alloys. The  $j_0$  parameter is presented here for the initial surface area and normalized to the true surface area of the catalyst.

Ref.#	$j_0/ \text{A cm}^{-2}$	Normalized $j_0/ \text{A cm}^{-2}$
26	$1.0 \times 10^{-3}$	$3.0 \times 10^{-6}$
35	-	$7.9 \times 10^{-5}$
36	$2.2 \times 10^{-3}$	$7.5 \times 10^{-6}$
37	-	$2.4 \times 10^{-6}$
38	$1.3 \times 10^{-2}$	$1.8 \times 10^{-6}$
39	$3.5 \times 10^{-3}$	-
40	$2.3 \times 10^{-2}$	-

#### 4. CONCLUSIONS

MoNi alloy deposit (at *ca.* 8.5 wt.%) on the surface of pure Ni foam material significantly boosted the catalytic activity of the baseline material towards hydrogen evolution reaction in alkaline media (mainly witnessed over kinetically-controlled overpotential range). The above is largely related to superior HER activity of a catalytic additive (MoNi alloy) over nickel element alone. Also, MoNi-modification results in a considerable increase of electrochemically active surface for this catalyst material.

Finally, the results obtained in this study showed considerable opportunities for Ni foam-modified cathode materials in commercial alkaline water electrolyzers.

#### References

1. B.E. Conway and B.V. Tilak, *Adv. Catal.*, 38 (1992) 1.
2. J.Y. Huot and L. Brossard, *Int. J. Hydrogen Energy*, 12 (1987) 821.
3. H.E.G. Rommal and P.J. Morgan, *J. Electrochem. Soc.*, 135 (1988) 343.
4. D.M. Soares, O. Teschke and I. Torriani, *J. Electrochem. Soc.*, 139 (1992) 98.
5. N. Krstajic, M. Popovic, B. Grgur, M. Vojnovic and D. Sepa, *J. Electroanal. Chem.*, 512 (2001) 16.
6. T. Hijikata, *Int. J. Hydrogen Energy*, 27 (2002) 115.

7. M. Momirlan and T.N. Veziroglu, *Int. J. Hydrogen Energy*, 30 (2005) 795.
8. R. Solmaz, *Int. J. Hydrogen Energy*, 38 (2013) 2251.
9. Z. Xie, P. He, L. Du, F. Dong, K. Dai and T. Zhang, *Electrochim. Acta*, 88 (2013) 390.
10. J.M. Olivares-Ramirez, M.L. Campos-Cornelio, J. Uribe Godinez, E. Borja-Arco and R.H. Castellanos, *Int. J. Hydrogen Energy*, 32 (2007) 3170.
11. M. Jafarian, O. Azizi, F. Gobal and M.G. Mahjani, *Int. J. Hydrogen Energy*, 32 (2007) 1686.
12. J.B. Yadav, J.W. Park, Y.J. Cho and O.S. Joo, *Int. J. Hydrogen Energy*, 35 (2010) 10067.
13. B. Pierozynski and L. Smoczynski, *J. Electrochem. Soc.*, 156 (2009) B1045.
14. B. Pierozynski, *Int. J. Electrochem. Sci.*, 6 (2011) 63.
15. B. Pierozynski, *Int. J. Hydrogen Energy*, 38 (2013) 7733.
16. R. Solmaz, A. Gundogdu, A. Doner and G. Kardas, *Int. J. Hydrogen Energy*, 37 (2012) 8917.
17. M.A. Dominguez-Crespo, E. Ramirez-Meneses, A.M. Torres-Huerta, V. Garibay-Febles and K. Philippot, *Int. J. Hydrogen Energy*, 37 (2012) 4798.
18. M. Mitov, E. Chorbadzhiyska, R. Rashkov and Y. Hubenova, *Int. J. Hydrogen Energy*, 37 (2012) 16522.
19. M.A. Dominguez-Crespo, A.M. Torres-Huerta, B. Brachetti-Sibaja and A. Flores-Vela, *Int. J. Hydrogen Energy*, 36 (2011) 135.
20. H. He, H. Liu, F. Liu and K. Zhou, *Surf. Coat. Technol.*, 201 (2006) 958.
21. E. Verlato, S. Cattarin, N. Comisso, A. Gambirasi, M. Musiani and L. Vazquez-Gomez, *Electrocatalysis*, 3 (2012) 48.
22. R. Diduszko, E. Kowalska, M. Kozlowski, E. Czerwosz and A. Kaminska, *Opt. Appl.*, XLIII(1) (2013) 133.
23. A. Lasia and A. Rami, *J. Appl. Electrochem.*, 22 (1992) 376.
24. L. Chen and A. Lasia, *J. Electrochem. Soc.*, 138 (1991) 3321.
25. H.J. Seim and M.L. Holt, *J. Electrochem. Soc.*, 96 (1949) 205.
26. M. Xia, T. Lei, N. Lv and N. Li, *Int. J. Hydrogen Energy*, 39 (2014) 4794.
27. B. Pierozynski, T. Mikolajczyk and I.M. Kowalski, *J. Power Sources*, 271 (2014) 231.
28. B. Pierozynski and T. Mikolajczyk, *Electrocatalysis*, 6 (2015) 51.
29. T. Pajkossy, *J. Electroanal. Chem.*, 364 (1994) 111.
30. B.E. Conway and B. Pierozynski, *J. Electroanal. Chem.*, 622 (2008) 10.
31. S-i. Tanaka, N. Hirose and T. Tanaki, *J. Electrochem. Soc.*, 146 (1999) 2477.
32. C. Gabrielli, F. Huet and R.P. Nogueira, *Electrochim. Acta*, 50 (2005) 3726.
33. J.A. Harrison, *Surf. Technol.*, 19 (1983) 249.
34. P. Paunovic, O. Popovski, S.H. Jordanov, A. Dimitrov and D. Slavkov, *J. Serb. Chem. Soc.*, 71 (2006) 149.
35. J.M. Jaksic, M.V. Vojnovic and N.V. Krstajic, *Electrochim. Acta*, 45 (2000) 4151.
36. J. Kubisztala, A. Budnioka and A. Lasia, *Int. J. Hydrogen Energy*, 32 (2007) 1211.
37. S. Shetty and A.C. Hegde, *Electrocatalysis*, 8 (2017) 179.
38. J. Panek, J. Kubisztal and B. Bierska-Piech, *Surf. Interface Anal.*, 46 (2014) 716.
39. A.W. Jeremiasse, J. Bergsma, J.M. Kleijn, M. Saakes, C.J.N. Buisman, M.C. Stuart and H.V.M. Hamelers, *Int. J. Hydrogen Energy*, 36 (2011) 10482.
40. E. Navarro-Flores, Z. Chong and S. Omanovic, *J. Mol. Catal. A: Chem.*, 226 (2005) 179.